Soft Wearable Augmented Walking Suit with Pneumatic Gel Muscles and Stance Phase Detection System to Assist Gait

Chetan Thakur[1] Kazunori Ogawa[1,2] Toshio Tsuji[1] Yuichi Kurita[1]

***Abstract*— The lower limbs of the human body are responsible for human locomotion and maintaining a good quality of life. However, there are many instances of muscle fatigue or injuries caused by stressful work environments, aging, and work that involves walking a long distance. Therefore, there is a need for an assistive suit for walking that can unload muscle efforts during walking and reduce the chances of lower-limb muscle fatigue. In this paper we discuss the development of a lightweight and wearable Augmented Walking Suit (AWS) using Pneumatic Gel Muscle (PGM) and its actuation control using lower limb pose detection mechanism considering the human gait cycle. The objective of this assistive suit is to reduce the required muscle effort of the posterior and anterior muscles during the swing phase of the gait cycle, thereby making it easier to move forward. To evaluate the effects of the AWS, an experiment was conducted to record the surface EMG (sEMG) of eight primary lower limb muscles of seven subjects for two levels of assistive air pressure. The evaluation was done based on the sEMG signal envelope and the statistical difference in the average percentage of maximum voluntary contraction (%MVC) of the measured muscles. In our result, we found that all muscles showed a statistically significant reduction or no change in muscle activity while wearing the AWS as compared with when the AWS was not worn.**

I. INTRODUCTION

The ability to move without interruption is one of the critical functions of the human body. It is one of the reasons for enjoying a good quality of life by performing a variety of daily tasks independently. However, there are many instances, such as aging, accidents, and longer and stressful working conditions that result in muscle fatigue and injuries, making it difficult to walk, thereby affecting the quality of life of the individual. Such situations can be avoided or addressed using exoskeletons or wearable assistive devices. The muscle activation pattern of human gait is dynamic, and it changes as the motion or intent is changed, but the basic pattern of the gait cycle remains. While developing the AWS, we considered factors such as the nature of the work area, age, flexibility for use it outdoors, light weight, portability, ease of use, reduced muscle effort during walking, and no impact on the normal gait cycle. With an increasing elderly population and stressful work conditions, devices like this will play a significant role in improving the quality of life. Garon et al. [1] mentioned that there is demand for assistive devices for mobility for people such as the elderly, the disabled, and healthcare staff for various tasks involved in daily life.

Among various lower-limb assistive devices, there is a tradeoff between autonomous actuation, wearability, light weight, and affordability. These are divided in two categories, exoskeletons and exosuits. In case of exoskeletons, HAL [2] makes walking easier for the elderly and supports rehabilitation for post stroke or accidents. Wearable agri robot [3] was designed for supporting farming activities and reduce muscle fatigue, it supports body posture and reduces the muscle fatigue. A walking assist device was designed for walking with a body weight support system [4] for augmenting walking and assisting the squatting motion required for pick-and-place tasks in various work environments. The RoboKnee [5] is one degree of freedom (DOF) exoskeleton designed to support human locomotion, such as walking and stair climbing. A plantarflexion assist exoskeleton [6] is designed to reduce the metabolic cost of walking.

In case of exosuits, a tethered bilateral hip extension and plantarflexion exosuit [7] was tested for assistance magnitude and changes in the metabolic cost of walking, and a reduction in metabolic energy by 22.8% while walking. A soft exosuit for hip assistance provides 30% of the biological torque moment for gait [8] by using a spooled-webbing actuator connected to the back of the thigh. The Myosuit, an untethered biarticular exosuit, reduces the natural knee extension moment during the sit to stand transfer motion by 26% [9]. Unilateral exosuit support for ankle plantarflexion and dorsiflexion were reported to reduce the metabolic rate of gait by 16% [10]. A soft inflatable exosuit for knee rehabilitation [11] reduces muscle activity in the rectus femoris by 7%. A biologically inspired soft exosuit for walking assistance [12] showed an average metabolic reduction of 5.1% during walking. A passive unpowered exoskeleton reduces metabolic cost of gait by 7% [13].

These devices are divided into segments, such as healthcare, disability support, and augmenting locomotion. These devices augment human motion significantly based on the reduction in EMG activities and metabolic rate during walking, but their use in outside environments is limited, especially in agriculture and factory settings. For augmented walking, wearability, light weight, portability, ease of use and reduced muscle fatigue, are essential but together missing in the assistive devices discussed above. To solve this problem, we previously developed a lightweight, low-powered pneumatic gel muscle (PGM) [14] as shown in Fig 1. The PGM can generate force with 60 kPa air pressure, which is not possible with the McKibben pneumatic artificial muscle (PAM) [15].

*The author (Chetan Thakur) was supported through the Hiroshima University TAOYAKA Program for creating a flexible, enduring, peaceful society, funded by the Program for Leading Graduate Schools, Ministry of Education, Culture, Sports, Science and Technology.

[1]Department of Systems Cybernetics, Graduate School of Engineering, Hiroshima University, Hiroshima, Japan

[2]Daiya Industries Co. Ltd. Japan

It is also structured to be stitched to fabric or fixed using Velcro tapes; this makes it easy to design the assistive suit. Fig 2 shows the relation of the supplied air pressure, generated force, and maximum elongation as a percentage of resting length.

In [16], we devised the concept of an unplugged powered suit (UPS) for walking assistance using the advantage of the PGM and the gait cycle. The UPS is a passive walking assist suit in which the air pressure required for actuating the PGM is generated by placing a rubber pump at the heel of the shoe. This configuration enables a limb in stance phase to generate the assistive air pressure required for the contralateral limb in the swing phase. The pump in the shoe can generate air pressure up to 50 kPa. The challenges of this configuration as discussed in [14], the UPS cannot be used for a walking pitch of faster than two steps per second. Another limitation of the UPS is the use of the pump in the shoe. To support multiple muscle groups, more pumps are needed in the shoe, which is not suitable for use in an outside environment because of possible leaks in the pump and the difficulty of walking with pumps in the shoe. In [14] evaluation of the UPS was done based on only four muscles of the lower limb, and only the rectus femoris showed a reduction in muscle activity by 20% whereas others showed no change. To overcome these challenges of the UPS, we developed the AWS in which an air tank replaces the pumps, and actuation control is designed using force sensitive resistor (FSR) sensors in the shoe. This change solves the problem of supporting variable walking speeds, providing the ability to support multiple muscle groups using additional PGM.

Here, we discuss the design and control of the AWS, which improves on the UPS by keeping human gait in the loop by using a gait cycle detection system for generating assistive force. In section II we discuss the PGM and its force characteristics, biomechanics, and human gait detection system, as well as the design and configuration of the AWS. In section III, we discuss the evaluation criteria, experimental method and setups, and results of the lower-limb sEMG evaluation for two levels of assistive force with the comparison of average gait sEMG envelope for all subjects and statistical analysis. Section IV presents the discussion, conclusion, and future works.

II. Methodology

A. Pneumatic Gel Muscle

The PGM is a type of PAM designed to be driven by low air pressure. Fig. 1 shows schematics and a prototype of the PGM. It has a resting length of 30 cm, maximum contraction length of 25 cm, and maximum elongation length of 45 cm. Construction of the PGM includes an inner tube made of a unique styrene-based thermoplastic elastomer to improve the flexibility, and an outer protective mesh. The McKibben PAM has rubber or silicone-based rubber tubes covered with protective mesh; these tubes need more air pressure to inflate, whereas the PGM can generate force with air pressure as low as 50 kPa and up to 300 kPa, as reported by [14]. The flexible design and ability to work with low air

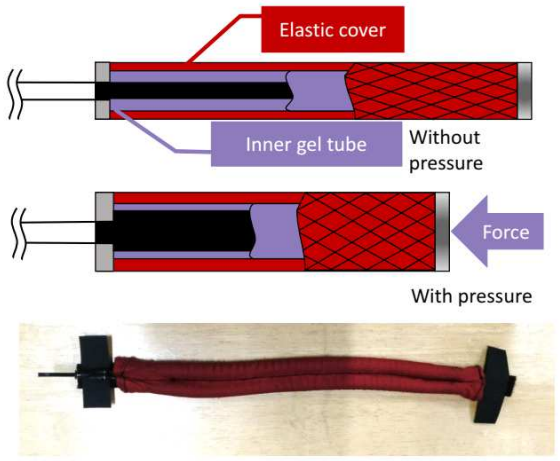

Fig. 1. Pneumatic Gel Muscle schematic and prototype. The inner gel tube can be inflated with low air pressure to generate required force. The resting length of the prototype is 30 cm.

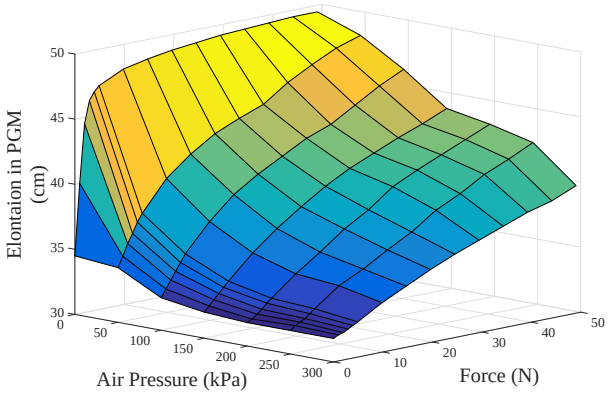

Fig. 2. The graph shows relationship of elongated length of PGM, air pressure and generated force as measured in [14].

pressure makes it a more suitable choice for development of wearable assistive suits than the McKibben PAM which has a higher force generating capacity but requires larger air pressure. Fig. 2 shows the elongation ratio of the PGM as measured by [14]. It shows the force-generating capacity of the PGM and elongation length for various levels of air pressure. In the experiment, one end of the PGM is fixed, and the test load is added to the other end. Whereas, in the AWS both ends of the PGM are fixed and stretched, in this case, the PGMs force-generating characteristics vary. This change is not measured in [14]. Therefore, we conducted an experiment to measure the force generated by the PGM for stretched and un-stretched conditions and different air pressures. The supported range of air pressure is 50 kPa to 300 kPa. Fig. 3 shows the experimental setup, where one end is connected to a load cell, and at the other end, the air source is connected through a Panasonic ADP5161 air pressure sensor. The experiment was conducted for two cases unstretched and stretched to 45 cm. Fig. 4 shows the

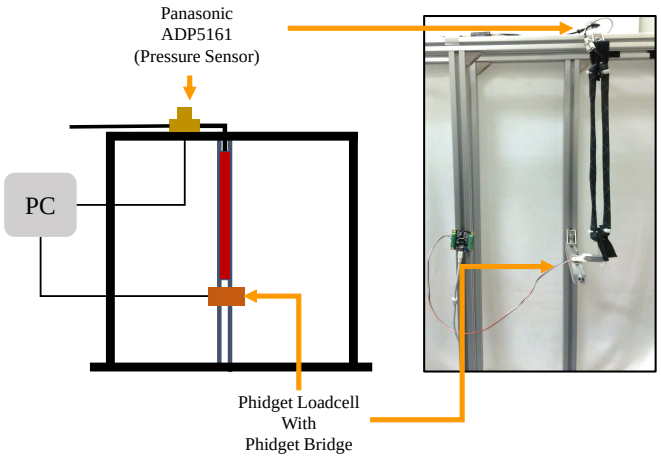

Fig. 3. Experiment setup for studying PGM's force profile.

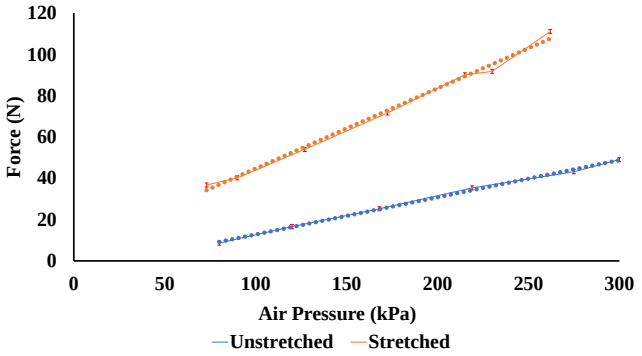

Fig. 4. PGM force profile for unstretched and stretched condition. This represents assistive force applied by PGM when used in AWS based on the input air pressure. In AWS the PGM is stretched along the length of the body segment it is attached. In our experiment we used 60 kPa and 100 kPa assistive air pressure for which approximately 30N and 44N of assistive force was applied by PGM based on the graph above.

measured force profile for two conditions in both cases, the PGM shows linear force generation characteristics that are modeled as a linear equations as described in equation 1 and 2 with their respective R^2 values. These models exhibit similar force generating behavior when used in AWS configuration. These characteristics are useful for controlling assistive force generated by PGM when used in the AWS.

$$y = 0.1799x - 5.1983; (R^2 = 0.993) \quad (1)$$

$$y = 0.3883x + 5.8899; (R^2 = 0.998) \quad (2)$$

B. Biomechanics of Gait Cycle

The design and control of the AWS are based on human walking, i.e., the gait cycle, and depend on how we walk. The gait cycle is divided into three major phases: stance phase, double limb support(DLS) phase and swing phase. The stance phase is responsible for weight acceptance and load transfer to support the swing phase of the contralateral limb. Fig. 5 shows the classification of the gait cycle in the stance and swing phases based on the orientation of the foot.

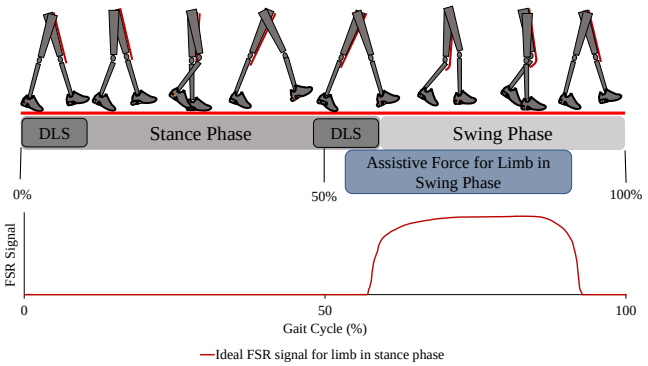

Fig. 5. The figure shows classification of gait cycle in stance and swing phase along with the double limb support (DLS) which occurs during transition from one phase to another. It also shows the region of assistive gait which starts during double limb support just before initial swing until terminal swing phase. The graph below shows ideal FSR signal from limb in stance phase which assist limb in sing phase.

During the transition from one phase to another, there always is a period when both the limbs are on the ground, this is the DLS. In the stance phase, muscle activation of the tibialis anterior (TA), rectus femoris (RF), vastus medialis (VM), vastus lateralis (VL), soleus (SOL), medial gastrocnemius (MG) and lateral gastrocnemius (LG) is observed. These muscles are active from heel strike until toe-off in the stance phase. In the DLS phase, the limb the transitioning in stance phase supports the forward locomotion of the contralateral limb going in the swing phase. In this phase, both the limbs are on the ground for approximately 10% of the one gait cycle. SOL, LG, MG, and RF muscles are active and responsible for the limb going into the swing phase. In the swing phase, the limb makes forward movement and RF, VL, VM, and biceps femoris (BF) are the major muscle contributors.

During the gait cycle, apart from the multiple muscle activation, the position and orientation of the foot also change. The orientation of the foot in the stance phase starts from the heel strike then flat foot, heel-off and ends with toe-off. However, in the swing phase, foot orientation starts from toe-off to heel strike. In DLS, the foot orientations of both limbs contrast with each other, i.e., one limb does heel strike and another does toe-off. This contrast information in DLS is helps to identify the limbs in swing and stance phase. In the AWS we used this information to design an assistive control mechanism to assist the swing phase of the gait cycle, which is discussed in the following subsection II-C.

C. AWS Design and Assistive Control Mechanism

AWS is designed to detect the gait cycle and as shown in Fig. 5 provide assistive force for the limb in the swing phase. To control the assistive force, we placed an FSR-406 sensor in the shoe to detect contrast foot orientation of both limbs in the DLS. The placement of the FSR sensors is shown in Fig. 6. This placement helps identify the change in foot orientation while transitioning from the stance to swing phase and vice versa in DLS. By utilizing the knowledge

Fig. 6. The figure shows FSR-406 pressure sensor placement in the shoe. This placement detects the limb in stance and swing phase during DLS

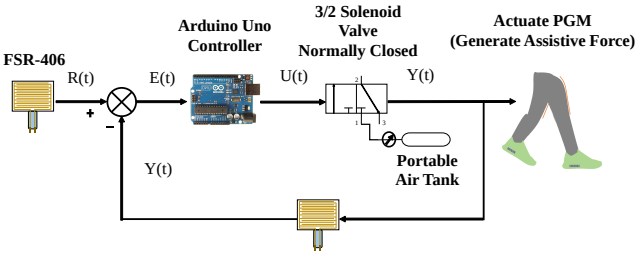

Fig. 7. The figure shows AWS assist control mechanism as a continuous process of Proportional (P) control which uses FSR sensor in the shoe to actuate PGM with pneumatic valves connected to portable air tank.

of the gait cycle and the foot orientation from the FSR, we designed the assistive control mechanism for the AWS. Fig. 7 shows the control mechanism of the AWS with the FSR-406 sensor-based stance and swing phase detection mechanism and assistive control. It is a continuous process of proportional (P) control where an Arduino Uno board monitors the FSR sensor data to identify the limbs in the stance and swing phase in the gait cycle. Detection of the limb in the swing phase triggers the assistive control mechanism of the PGM. For actuation control, we used a Kaganei G010E1 3/2 normally closed solenoid valve. The FSR sensor data are continuously monitored for switching ON/OFF solenoid valves. This system is realized using following equation

$$E = R - Y \tag{3}$$

$$U = kpE \tag{4}$$

where E is error signal, R is the calibrated threshold value of the FSR sensor, Y is the analog value of the FSR sensor, U is the input to the solenoid valve, and kp is the P-gain.

The assistive-control mechanism detects the gait cycle by sensing the transition from one phase to another on both limbs in DLS. This way, we avoid unwanted assistive forces during the stationary state where there is no transition. The assistive force generated by the AWS is directly proportional to the supplied air pressure. The supplied air pressure is controlled using the regulator attached to a small air tank used as a source of air pressure.

Fig. 8 shows the developed prototype of AWS. AWS consists of waist support and knee support belt for fixing the PGM, PGM along rectus femoris of both limbs, solenoid

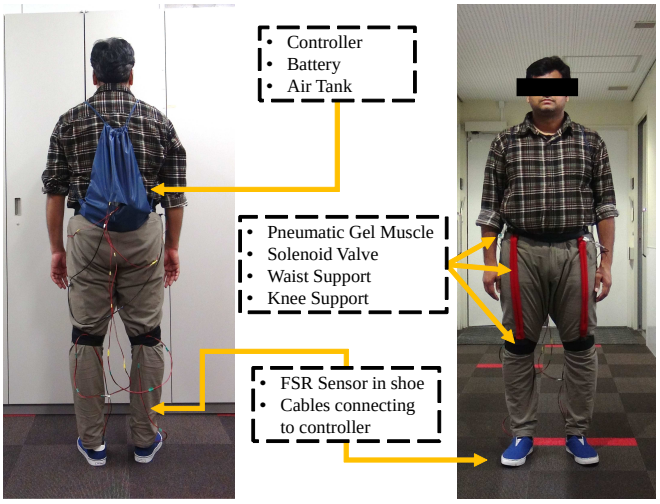

Fig. 8. The figure shows a subject wearing proposed AWS. The suit consists of backpack with controller, battery and air tank, waist support belt, knee support, two PGMs, pneumatic valves, pressure sensors placed in shoe for controlling assistive force.

TABLE I
TOTAL WEIGHT OF AWS AND ITS INDIVIDUAL PARTS.

Part Name	Numbers	Weight (kg)
Air Tank with Regulator	1	0.582
Solenoid Valve	2	0.040
PGM	2	0.110
Tubes	1	0.022
Knee Support Belt	2	0.052
Waist Support Belt	1	0.108
Controller and wires	1	0.303
Total		1.217

valves connected to the PGM for actuation control, drawstring backpack which has controller circuit, portable battery and portable air tank. FSR sensors in the shoes are connected to the controller using wires. The weight of the system is 1.2 kg which is lighter than most of the state of the art wearable and portable walking assistive suits. Table I shows weights of individual components used in AWS along with total weight of the system.

III. AWS PERFORMANCE EVALUATION THROUGH MUSCLE ACTIVATION PATTERN OF LOWER-LIMB MUSCLES

To test our assumption that the newly developed AWS can assist walking and that change in assistive air pressure reduces muscle activity in lower-limb muscle groups the experiment was conducted to test the performance evaluation of the AWS with two levels of assistive air pressure.

Walking involves a combination of muscle activation dynamics of the anterior and posterior lower limb muscles. These changes were recorded using sEMG signals of eight major posterior and anterior muscles that contribute to the gait cycle. We measured TA, SOL, MG, LG, RF, VM, VL, and BF. These muscles are superficially accessible to record sEMG of the lower limb and collectively support the gait

cycle. The performance of the AWS is measured based on the statistical difference in the sEMG recorded when the subject was not wearing the AWS and wearing the AWS with two levels of assistive air pressure.

A. Experiment Protocol

To evaluate the effect of the AWS on the muscle activation pattern of lower-limb muscles for two levels of assistive air pressure, the device was tested on a group of seven healthy young subjects with no gait abnormalities. The subjects age ($\pm$ SD) was 28.8 $\pm$ 5.1, height was 150 $\pm$ 10 cm, and weight was 70.8 $\pm$ 14.5 kg. All the subjects participated in the experiment after a brief introduction of the AWS and experiment requirements.

For effective evaluation of the assisted gait, we need to measure a minimum of three full gait cycles [17]. In our experiment, we recorded sEMG for ten full gait cycles. This was done by asking subjects to walk 15 m straight on a flat surface by maintaining the walking speed during all experiments. The sEMG and FSR sensor data were logged using Personal EMG (P-EMG) device from Oisaka electronic Ltd. For continuous and uninterrupted walking and recording of the data during the experiment, we prepared a backpack containing the P-EMG device, portable battery, and a laptop to operate the P-EMG device. The backpack also contained a controller circuit for the AWS and portable air tank. The laptop was accessed remotely to record the sEMG. Fig. 9 shows the experimental setup with the backpack. The total weight of the backpack during experimental evaluation was 6 kg.

With the above setup, we conducted three experiments to evaluate the AWS. In the first, sEMG data were recorded for a normal gait, i.e., when subjects were not wearing the AWS. This data gave us the baseline for evaluating the effects of the AWS. In the second and third experiments, sEMG data were recorded for the assisted gait, i.e., subjects wearing the AWS with the backpack containing the experimental setup. For all subjects sEMG of right limb was measured for two levels of assistive air pressure during this experiment, i.e. 60 kPa and 100 kPa respectively. Three iterations of each experiment were performed to record enough data to conduct a statistical analysis.

B. Results

The recorded sEMG was rectified with integrated EMG (iEMG), a second-order low-pass filter with a cut-off frequency of 100 Hz, and a second-order high-pass filter with a cut-off frequency of 40 Hz using the P-EMG plus tool for the P-EMG device. The recorded sEMG was normalized using MVC to find %MVC, and ten gait cycles for each subject were averaged to create one gait cycle which is further averaged to generate one gait cycle of all subject. The segmentation of gait cycle was done from stance to stance detection on the left limb based on FSR sensor data in P-EMG tool. This was done because stance phase of one limb assists swing phase of the contralateral limb. We measured standard deviation and performed statistical analysis using a two-sample t-test on the average normalized sEMG for all muscles under observation.

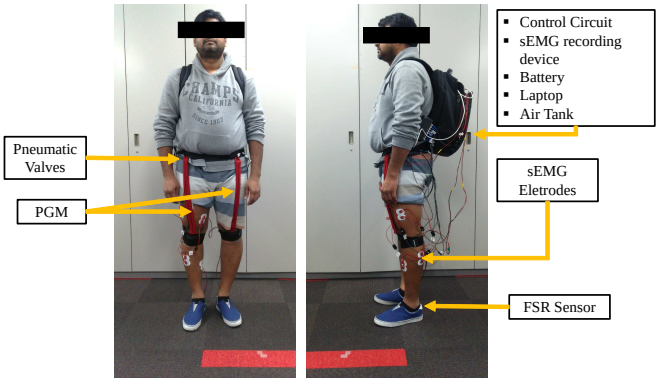

Fig. 9. Experiment setup, subject wearing AWS, electrodes and backpack. The backpack contains sEMG recording device, laptop, controller for the AWS, portable battery for controller and sEMG recording device. The total weight of the backpack is 6 kg.

Fig. 10 shows the normalized average sEMG signal envelope for all subjects with standard deviation of the gait cycle without wearing AWS and wearing AWS with two levels assistive air pressure at 60 kPa and 100 kPa. The gait cycle reference for the sEMG signal is swing to swing phase of the right limb.The figure also shows the FSR sensor data for both limbs. The signal peak shows the stance phase on the respective limb and swing on the contralateral limb. AWS detects stance phase on the left and assists swing phase of the right limb (during the experiment we measured sEMG of the right limb). From the graphs, we see that, as we increase the assistive air pressure reduction in the peak value of the normalized averaged sEMG signal not only in the swing phase but also in the stance phase. To evaluate the differences quantitatively, we conducted a two-sample t-test between unassisted gait when AWS was not worn and assisted gaits. Fig. 11 shows averaged %MVC for the three experiments and their significance for individual muscles.

All the muscles showed significant reduction or no change in the muscle activity evaluated during the experiment. Muscles showed reduction for both levels of assistive air pressure. Table II shows the result of the two-sample t-test showing the significance of the reduction in the muscle activity based on $p - value$. The Table III shows percentage reduction in muscle activity. TA, LG, RF, VL and BF shows larger reduction in %MVC while for SOL, MG and VM shows reduction less than 10% of %MVC. From the data in both the tables we observe that assisting swing phase by controlled actuation reduces muscle activity of the measured muscles of the lower limb.

Therefore, based on the results and analysis we found that the AWS developed in this study can augment human gait as compared to when no AWS is worn. The AWS was able to reduce the muscle efforts significantly in both levels of assisted by assisting swing phase of the gait cycle.

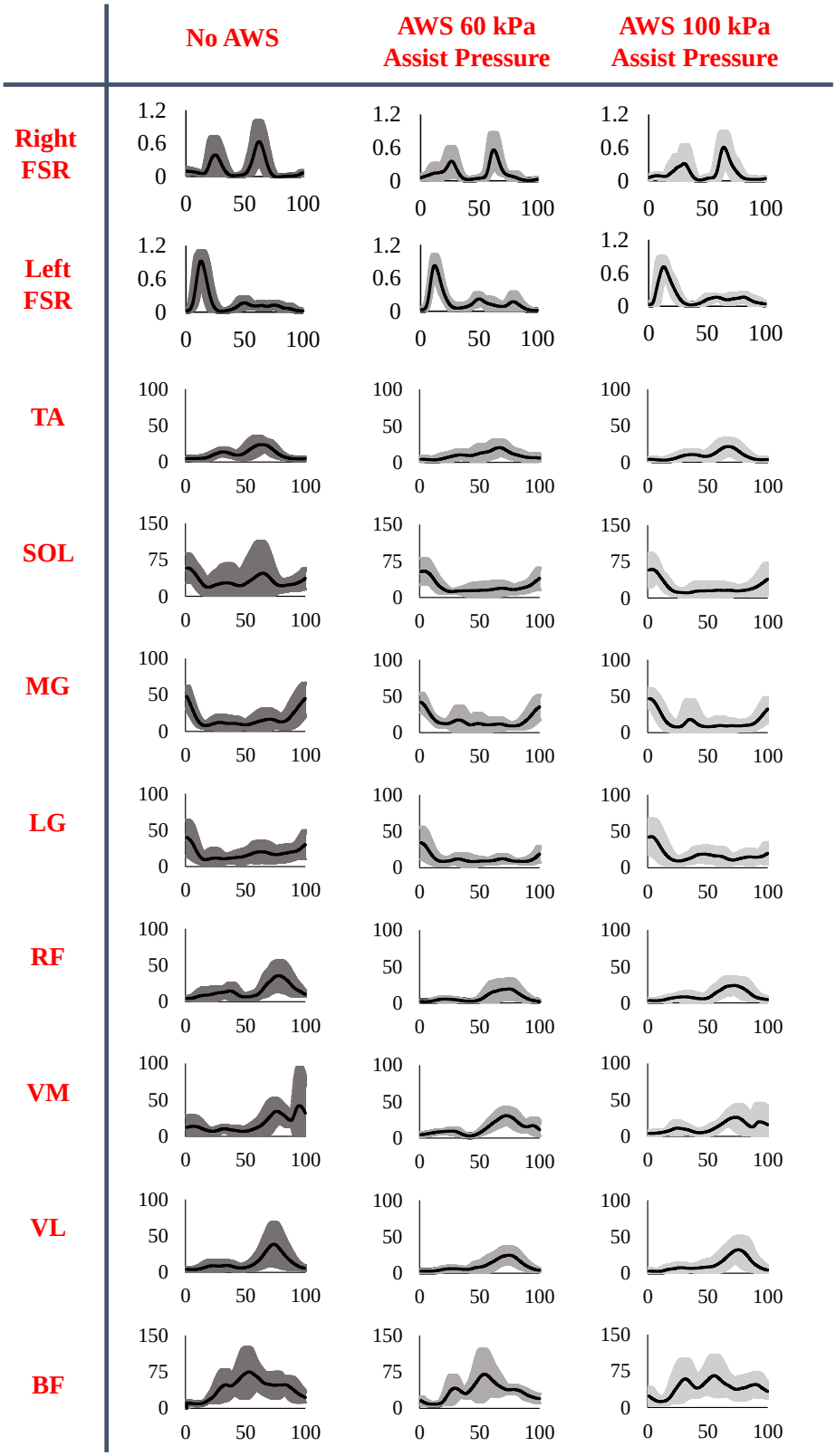

Fig. 10. The figure shows normalized averaged sEMG signal envelope for lower limb muscle groups observed for walking when AWS is not worn and when AWS is worn with two levels of assistive air pressure. It also shows FSR sensor signal showing assistive phase in the gait cycle. The X-axis is the percentage gait cycle (heel strike to heel strike). The Y-axis of the FSR signal is voltage out recorded on the P-EMG device, and for the muscle group, it is average percentage MVC recorded during the experiment.

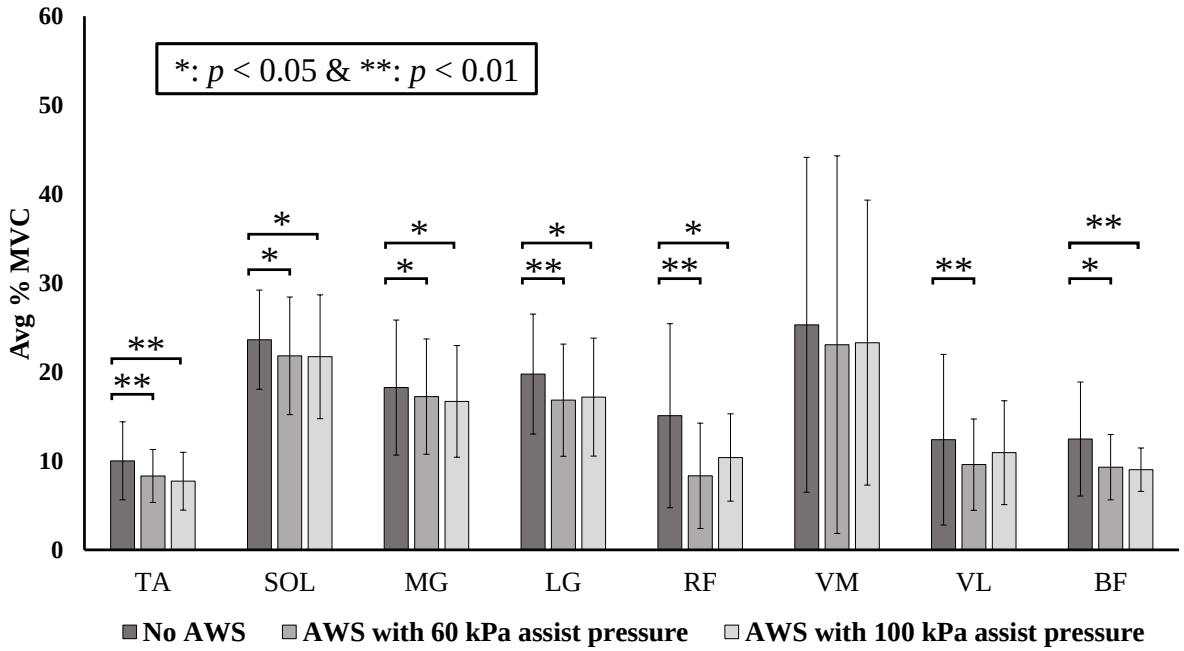

Fig. 11. The figure shows the significance of the reduction in %MVC of the muscle groups for unassisted and assisted with two level of assistive force. The result shows significant reduction or no change in the muscle activation during assisted walking recorded for seven subjects.

TABLE II

RESULT OF TWO SAMPLE T-TEST WITH THE RESPECTIVE P-VALUE, T-VALUE AND T-CRITICAL. P-VALUES ARE MARKED WITH * (< 0.05) OR ** (< 0.01) AS DISPLAYED IN FIG. 11.

Muscles	Experiment	*p-value*	*t-value*	*t-critical*
TA	AWS 60 Kpa	0.0001 **	14.51	2.78
	AWS 100 Kpa	0.0002 **	24.25	3.18
SOL	AWS 60 Kpa	0.0392 *	3.02	2.78
	AWS 100 Kpa	0.0329 *	3.20	2.78
MG	AWS 60 Kpa	0.0310 *	3.85	3.18
	AWS 100 Kpa	0.0116 *	4.41	2.78
LG	AWS 60 Kpa	0.0095 **	4.68	2.78
	AWS 100 Kpa	0.0201 *	4.53	3.18
RF	AWS 60 Kpa	0.0079 **	6.35	3.18
	AWS 100 Kpa	0.0420 *	4.72	4.30
VM	AWS 60 Kpa	0.0670	2.50	2.78
	AWS 100 Kpa	0.3300	1.16	3.18
VL	AWS 60 Kpa	0.0075 **	6.46	3.18
	AWS 100 Kpa	0.4003	1.06	4.30
BF	AWS 60 Kpa	0.0192 *	7.11	4.30
	AWS 100 Kpa	0.0020 **	10.16	3.18

IV. DISCUSSION

Our results show that the previously developed PGM can be used for the development of the AWS and make it lightweight, portable, and easy to use. The use of the AWS showed a reduction in the muscle activity in all the major lower-limb muscles. Because of the soft nature of the suit this device does not drastically disturb the normal gait of the wearer.

The assistive control developed for the AWS detects limbs going in the stance and swing phase during DLS by sensing the FSR sensor data. The simple P control supports 20%-30% of the gait cycle during the swing phase. Because of the nature of the gait cycle and power source for the actuator, it is easy to add additional PGMs to the AWS for increasing the range of the assistive force. It is also possible to support the stance and swing phase on a contralateral limb using same solenoid valve, since in the standard gait cycle both limbs functions synchronously. The device uses waist and knee support to attach the PGM along the rectus femoris muscle. This position sometimes a causes little disturbance during walking. It can be addressed by changing the way PGMs are attached to the limbs in such a way such that it does not disturb the degree of freedom at the knee or any other joint when the PGMs are used.

State-of-the-art wearable walking assist suits are inspired by the biological function of walking, and the assistive actuators aligned with the muscles and joints of the lower limb [8] .. [13]. In such devices, the swing phase of the gait is assisted with an actuators attached close to the ankle or along the soleus muscle and a reduction in the metabolic cost of walking is demonstrated. In our research, AWS is developed to assist the swing phase PGM is attached along the RF muscle from hip to knee, and experimental evaluation shows a progressive reduction in the muscle activity of TA, SOL, MG, and LG. Along with this, RF, VL, and BF also show a reduction in muscle activity.

Qualitatively, from the oral feedback from subjects, we found that the device is lightweight when not using the 6 kg experimental setup; subjects also reported feeling the assistive force of the PGM during the swing phase of the gait cycle. Some subjects reported feeling assistive force during walking when assistive air pressure changed to 100 kPa as compared to 60 kPa. They also reported that the PGM attachments do not disturb the walking experience but

TABLE III
REDUCTION IN %MVC DURING ASSISTED WALKING.

Muscle	60 kPa Assistive Force	100 kPa Assistive Force
TA	16.90%	22.70%
SOL	7.70%	8.10%
MG	5.50%	8.50%
LG	14.84%	13.10%
RF	44.00%	31%
VM	8.80%	7.90%
VL	22.50%	11.70%
BF	25.40%	27.60%

improving the attachment at the knee can result in a more comfortable walking experience.

V. CONCLUSION AND FUTURE WORK

In this paper, we discussed the design, development, and evaluation of the AWS to overcome the limitations of the UPS regarding variable walking speed, ease of use, and portability. To achieve this, we developed an assistive control system by detecting limbs in the stance and swing phase during the DLS phase of the gait cycle. The simple P control can switch on / off the assistive force during the swing and stance phase respectively. While transitioning from the UPS to AWS, the device weights 1.2 kg due to use of portable air tanks. We demonstrated the ability to unload muscle efforts significantly by two levels of assistive force by the AWS (comparing the sEMG when not wearing AWS and when wearing AWS).

Our evaluation shows the AWS unloads muscle efforts during walking. During this process, we found many areas for improvements and future work. In our result, we observe antagonistic behavior for RF, VM, VL, and BF. Increase in the assistive air pressure decreases reduction in muscle efforts; we intend to search for the cause of such behavior in our further research and find the mechanism to cancel out such behavior. In our current study, we evaluated the AWS using muscle activity changes, but kinematic and physiological studies is also essential for the evaluation of wearable assistive suits; thus, we plan to conduct these studies in the future. The assistive control of the AWS uses FSR sensors in the shoe, the wires connecting from the shoe to the controller in the backpack cause a little irritation to the user. FSR sensors are sensitive to applied pressure, in our experiment we observed the right FSR always shows activity in the swing phase of the gait cycle. However, since the peak value is less than the stance threshold, therefore, this does not interfere in the actuation control of the AWS. We think, detailed lower limb assist control can be achieved by the use of inertial measurement unit (IMU) sensors at the knee and ankle joint or flexible stretch sensors which provide more significant information regarding the gait cycle. In the current implementation of the AWS, a backpack is used to keep the controller, battery, and air tank. In the future, we want to integrate these in the waist support belt to make the device more user-friendly and comfortable to wear. We believe devices like these have much promise for augmenting human walking for various age groups, rehabilitation and augmented sports and fun activities. Our further activities involve modeling of PGM force characteristics and using it for dynamic assistive control and canceling out the adverse effect on some of the muscle.

ACKNOWLEDGMENT

The authors take this opportunity to thank members of Biological Systems Engineering lab at Graduate School of Engineering in Hiroshima University, Japan for participating in the performance evaluation of the AWS. We also like to thank Daiya Industries for supply and support for PGM development.

REFERENCES

[1] L. Garon et al., Medical and assistive health technology: Meeting the needs of aging populations, Gerontologist, vol. 56, pp. S293S302, 2016.
[2] K. Suzuki, G. Mito, H. Kawamoto, Y. Hasegawa, and Y. Sankai, Intention-based walking support for paraplegia patients with Robot Suit HAL, Adv. Robot., vol. 21, no. 12, pp. 14411469, 2007.
[3] S. Toyama and G. Yamamoto, Development of wearable-agri-robot - Mechanism for agricultural work, in 2009 IEEE/RSJ International Conference on Intelligent Robots and Systems, IROS 2009, 2009, pp. 58015806.
[4] Y. Ikeuchi, J. Ashihara, Y. Hiki, H. Kudoh, and T. Noda, Walking assist device with bodyweight support system, in 2009 IEEE/RSJ International Conference on Intelligent Robots and Systems, IROS 2009, 2009, pp. 40734079.
[5] J. E. Pratt, B. T. Krupp, C. J. Morse, and S. H. Collins, The RoboKnee: an exoskeleton for enhancing strength and endurance during walking, in IEEE International Conference on Robotics and Automation, 2004. Proceedings. ICRA 04. 2004, 2004, vol. 3, p. 24302435 Vol.3.
[6] P. Malcolm, W. Derave, S. Galle, and D. De Clercq, A simple exoskeleton that assists plantarflexion can reduce the metabolic cost of human walking, PLoS One, vol. 8, no. 2, 2013.
[7] B. T. Quinlivan et al., Assistance magnitude versus metabolic cost reductions for a tethered multiarticular soft exosuit, Sci. Robot., vol. 2, no. 2, p. eaah4416, 2017.
[8] A. T. Asbeck, K. Schmidt, and C. J. Walsh, Soft exosuit for hip assistance, Rob. Auton. Syst., vol. 73, pp. 102110, 2015.
[9] K. Schmidt et al., The Myosuit: Bi-articular anti-gravity exosuit that reduces hip extensor activity in sitting transfers, Front. Neurorobot., vol. 11, no. OCT, pp. 116, 2017.
[10] L. N. Awad et al., A soft robotic exosuit improves walking in patients after stroke, Sci. Transl. Med., vol. 9, no. 400, 2017.
[11] S. Sridar, P. H. Nguyen, M. Zhu, Q. P. Lam, and P. Polygerinos, Development of a soft-inflatable exosuit for knee rehabilitation, in 2017 IEEE/RSJ International Conference on Intelligent Robots and Systems (IROS), 2017, pp. 37223727.
[12] A. T. Asbeck, S. M. M. De Rossi, K. G. Holt, and C. J. Walsh, A biologically inspired soft exosuit for walking assistance, Int. J. Rob. Res., vol. 34, no. 6, pp. 744762, 2015.
[13] S. H. Collins, M. B. Wiggin, and G. S. Sawicki, Reducing the energy cost of human walking using an unpowered exoskeleton, Nature, vol. 522, no. 7555, pp. 212215, 2015.
[14] K. Ogawa, C. Thakur, T. Ikeda, T. Tsuji, and Y. Kurita, Development of a pneumatic artificial muscle driven by low pressure and its application to the unplugged powered suit, Adv. Robot., vol. 31, no. 21, pp. 11351143, 2017.
[15] F. Daerden and D. Lefeber, Pneumatic artificial muscles: actuators for robotics and automation, Eur. J. Mech. Environ. Eng., vol. 47, no. 1, pp. 1121, 2002.
[16] C. Thakur, K. Ogawa, T. Tsuj, and Y. Kurita, Unplugged powered suit with pneumatic gel muscles, in Lecture Notes in Electrical Engineering, 2018, vol. 432, pp. 247251.
[17] R. W. Kressig and O. Beauchet, Guidelines for clinical applications of spatio-temporal gait analysis in older adults, Aging Clin. Exp. Res., vol. 18, no. 2, pp. 174176, Apr. 2006.